HYDRODYNAMIC PRESSURE GENERATED BY DOCTORING IN BLADE GAP FORMERS

Alireza Roshanzamir, Carl Ollivier-Gooch, Richard J. Kerekes, and Sheldon I. Green

Department of Mechanical Engineering
and Pulp and Paper Centre
University of British Columbia
Vancouver, BC, Canada

ABSTRACT

Water adhering to the blade-side of a fabric in a gap former is deflected or "doctored" by the blades. The pressure distribution generated in this process and its effects on the pressure pulses in the gap between fabrics has been studied. The thickness of the adhering water layer was first estimated using a one-dimensional model. Next, a free-surface model was used to find the pressure distribution in the water layer close to the blade. The pressure distribution acting on the blade-side of the fabric was then applied as a new boundary condition in a previously developed two-dimensional model of the flow within the gap. The complete model predicted that, in the doctoring process, the pressure in the water layer reached its stagnation value some small distance away from the fabric–blade contact point, toward the blade support. Under typical paper machine conditions, the pressure acting on the fabric from the stagnation zone was found to be about 50% of the stagnation point pressure. The size of the zone over which the pressure extended was a few millimeters. This pressure increased the pressure between the fabrics by 30% to 100%, depending on the radius of curvature of the blade edge. The stagnation zone pressure also forced some water back into the gap between the fabrics, but the amount was small, only about 10% of the drained water.

INTRODUCTION

Over the past few years, a number of studies have been carried out to model pressure pulses in blade gap formers *(1–6)*. In all blade gap formers, dewatering produces a thin water layer adhering to the surface of the moving fabrics. Blades "doctor" or deflect this water layer on the blade-side fabric, as mentioned by Norman *(7)*. During this process, a pressure distribution is generated in the water layer very close (on the order of a few millimeters) upstream from the leading edge of the blade. This pressure distribution is called the "doctoring pressure."

As a first approximation, in a one-dimensional model of blade gap forming, Green and Kerekes *(2)* represented the doctoring pressure distribution by an exponential function. According to their prediction, for a thin blade, the peak pressure pulse within the gap would increase by 50% under typical operation conditions because of the doctoring pressure. For a finite-width blade, under the same conditions, the peak pressure pulses might increase even more. Owing to the passage of water through the forming fabric and the radius of curvature of the blade tip (nose radius), the location of the stagnation pressure, p_0, will be some small distance away from the contact point between the fabric and blade. As a result, one could anticipate that the effect of doctoring pressure on pressure pulses is less than that predicted previously.

The objective of this study was to determine the doctoring pressure distribution and to investigate its effect on pressure pulses developed between the fabrics in gap forming for some practical blade geometries.

ANALYSIS

Figure 1 shows a schematic of a single-blade former and some physical parameters involved in the problem. As the pulp suspension approaches the blade, the suspension velocity decreases, its pressure increases, and dewatering takes place. Complete one-dimensional and two-dimensional analyses of a single-blade former are given in previous works *(2, 3)*. In the two-dimensional model that neglects the doctoring pressure, a constant-pressure boundary condition was applied on the blade side of the fabric. This boundary condition must be modified to reflect the doctoring pressure distribution close to the blade. In order to develop a mathematical model for this process, the following assumptions are made:

1. The pulp suspension behaves as a Newtonian fluid.
2. Darcy's Law can be used to model the flow through the fabrics.
3. The permeability of the fiber and mat is constant.
4. The water layer moves with the same velocity as the fabric far upstream of the blade.
5. The water layer contains no fibers and additives (i.e., retention is 100%).
6. The fabrics have no stiffness.
7. The bottom fabric follows the shape of the blade surface.

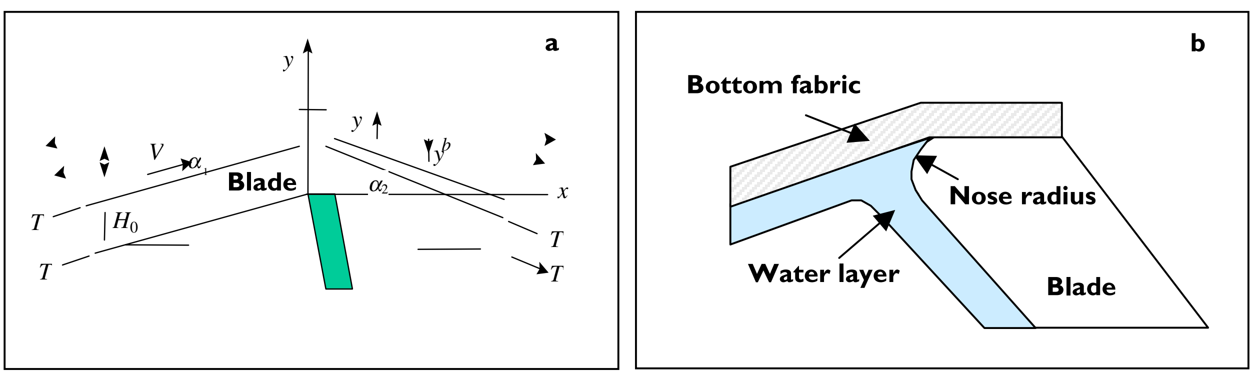

Figure 1. Schematic of a single-blade gap former (a) and the region close to the blade, where water is doctored by the blade (b).

Method of solution

This complex free-surface flow is solved iteratively. In the first step, a one-dimensional analytical model is solved to estimate the pressure distribution and fabric separation without considering the effect of doctoring pressure. This model was previously developed based on a linearization approach *(1)* to derive two ordinary differential equations whose solutions are the pressure pulses upstream and over a finite-width blade. The variables used are given in **Table I**:

Tension on fabrics (T)	8,000 N/m
Velocity of fabrics (V)	14 m/s
Wrap angles ($\alpha_1 = -\alpha_2$)	1°
Upstream gap size (H_0)	3.5 mm
Average fiber+mat resistance (R)	20,000 Pa•s/m
Blade width (s)	40 mm

Table I. Fixed variable used in simulations.

In the next step, the thickness of the water layer approaching the blade, h_w, is estimated by integrating the dewatering velocity upstream to somewhere close to the blade (x_0, taken as a few times the water layer thickness). Since the dewatering velocity is $W_1 = p/R$, where R is the drainage resistance and p is the local pressure in the gap, the water film thickness is:

$$h_w = \frac{\int_{-\infty}^{x_0} p\,dx}{VR}$$

In order to determine the distance over which the doctoring pressure applies, the inviscid theory of flow around a corner can be used. According to this theory, the pressure applies over a distance about 4–5 times the fluid thickness. Considering the low viscosity of water and the high velocity of the water layer relative to the blade, the inviscid theory should be qualitatively correct. We use this theory to select x_0 and define the domain in which two-phase flow modeling is done.

Given knowledge of the velocity and thickness of the water layer approaching the blade, the Volume of Fluid (VOF) model *(8)* is employed to find the doctoring pressure in the region close to the blade. Such VOF models are commonly used to model two or more immiscible fluids. For each additional phase, the volume fraction of that phase is introduced as a variable. In each cell volume in the domain, the volume fractions of the two phases add to unity. If the volume fraction of the k^{th} fluid in a multiphase flow is denoted ε_k, then:

$\varepsilon_k = 0$ — the cell is empty of the k^{th} fluid
$\varepsilon_k = 1$ — the cell is full of the k^{th} fluid
$0 < \varepsilon_k < 1$ — the cell contains the interface between the fluids

The properties and variables are assigned to each cell, based on the local value of ε_k. The tracking of the interfaces between the N phases is accomplished by the solution of a continuity equation for the volume fraction of N–1 phases:

$$u_j \frac{\partial \varepsilon_k}{\partial x_i} = 0$$

In our system, air and water are the two fluids. The properties (e.g., density and viscosity) in the transport equations are determined based on the amount of each phase present in each control volume, for example:

$$\rho = \varepsilon_{\text{water}} \rho_{\text{water}} + (1 - \varepsilon_{\text{water}}) \rho_{\text{air}}$$

The fluids share a single set of momentum equations.

$$\frac{\partial}{\partial x_i} \rho u_i u_j = -\frac{\partial p}{\partial x_j} + \frac{\partial}{\partial x_i} \mu \left(\frac{\partial u_i}{\partial x_j} + \frac{\partial u_j}{\partial x_i} \right)$$

The FLUENT CFD code is used to solve the VOF model. **Figure 2** shows a typical free-surface profile and a pressure contour obtained from the VOF model. Boundary conditions used in this modeling are given in **Table II**.

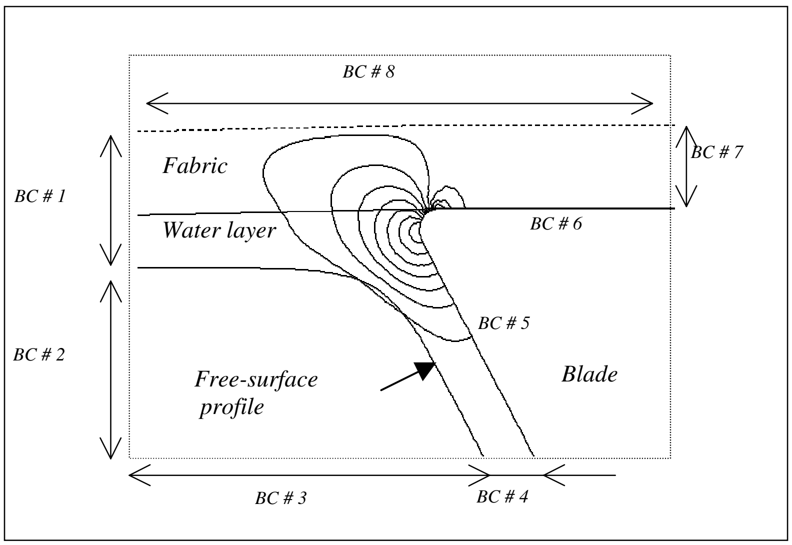

Figure 2. A typical free-surface profile and pressure contours obtained from the VOF model. One pressure contour crosses the free surface owing to the definition of the water–air interface location, which is based on the local value of ε_k.

Boundary condition	Normal velocity	Static pressure	Volume fraction of water
1	√ constant	…	1
2	…	√ constant	0
3	…	√ constant	0
4	…	√ constant	1
7	…	√ constant	1
8	…	√ profile	1

Table II. Boundary conditions used in the VOF model.

Boundary conditions on 5 and 6 are for walls with no slip and slip, respectively. The solution is considered converged when residuals fall below 5×10^{-4}.

The doctoring pressure changes the pressure pulses obtained in step one, and therefore an iterative method is necessary to correct the pressure pulses and the resulting doctoring pressure. Iteration continues until the pressure pulses and the resultant doctoring stop changing significantly from one iteration to the next (normally 2–3 iterations). After finding the right doctoring pressure from the VOF model, the doctoring pressure is then applied as a new pressure boundary condition in the two-dimensional model of within-gap flow. Details of this model were described by Roshanzamir *et al.* *(3)*. (Figure 4 shows a typical pressure distribution in the gap upstream of and over a finite-width blade obtained from the one-dimensional model.)

Finally, the doctoring pressure used in the two-dimensional model can be checked by applying the pressure on the bottom fabric as a boundary condition (BC No. 8) in the VOF model.

Comparison of VOF simulation with inviscid theory

In order to test the accuracy of the VOF model, we assume that the resistance of the fiber mat and fabric approaches infinity and the sum of the wrap angle and the blade angle is 90°. Physically, this means that we replace the fabric with a solid wall. **Figure 3** shows the computed pressure distribution acting on the upper wall for a 0.5-mm-thick water layer approaching a corner. The water layer approaches the corner with a velocity at 14 m/s. The agreement between the analytical results *(9)* and the VOF modeling is very good, which lends support to the use of VOF modeling for the blade-doctoring problem.

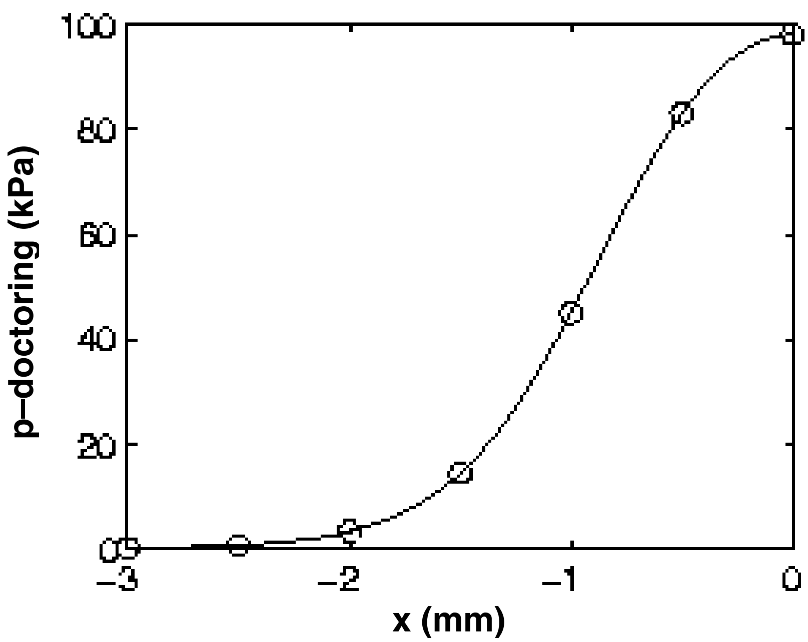

Figure 3. Pressure distribution along upper wall. The circles represent inviscid theory results (9).

RESULTS

We first examine the effect of the blade nose on the doctoring pressure, and then the effect of doctoring on the pressure pulse.

2-D free-surface model: Effect of nose radius on doctoring pressure

In order to study the effect of blade nose radius on the doctoring pressure, a number of blades were considered. **Table III** shows the blade characteristics used in the simulations.

Blade No.	Nose radius, mm
1	0
2	0.254
3	0.635
4	1.016

Table III. Geometry of forming blades.

Figures 4 and 5 show the pressure and volume-fraction contours for Blade 2. The thickness of the water layer is 0.5 mm and moves at 14 m/s upstream of the blade. As shown in Figure 4, the location of the stagnation pressure, p_0, is some small distance away from the contact point between the fabric and blade, which is expected owing to the porosity of the forming fabric. A very small region of negative pressure is apparent near the location where the fabric wraps around the blade tip. This negative pressure is caused by bending of streamlines in the flow.

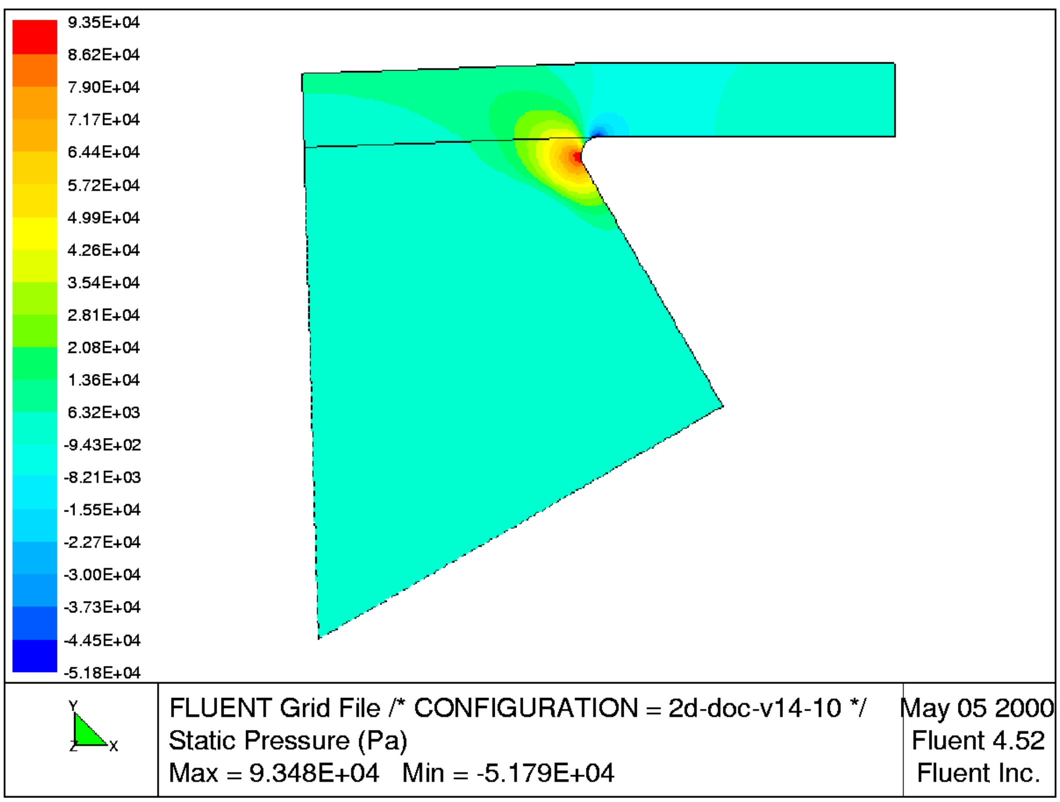

Figure 4. Pressure contours for Blade 2 (pressure expressed in units of Pascals).

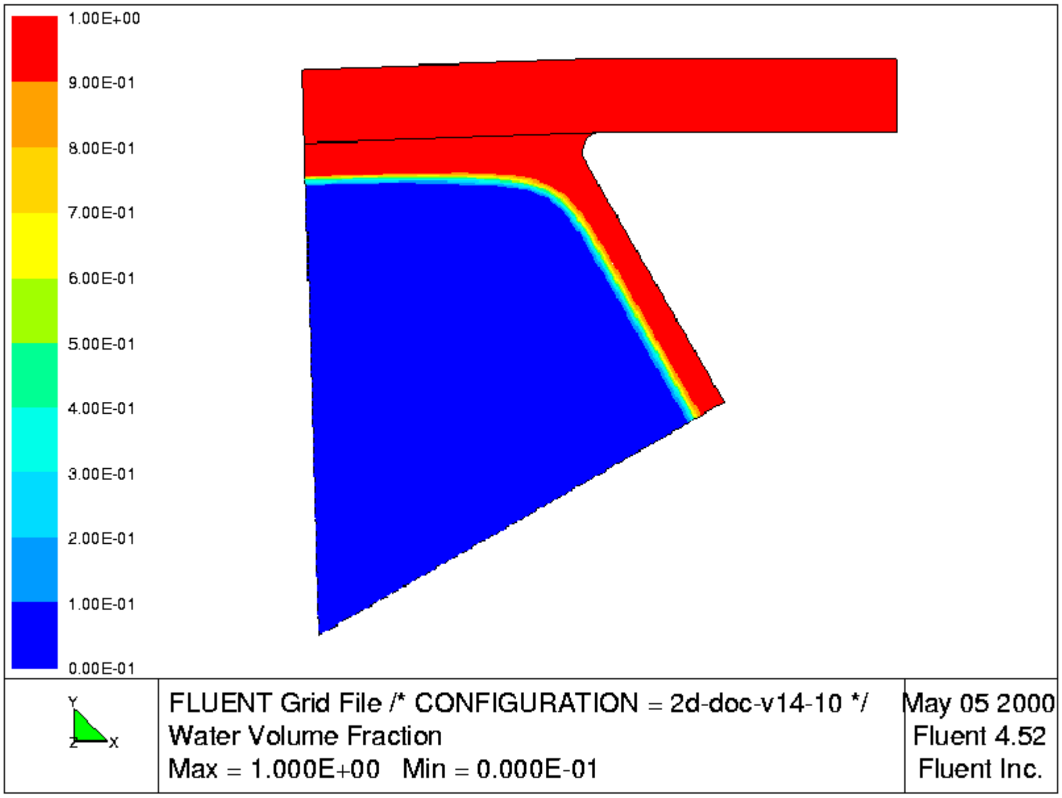

Figure 5. Volume fraction of water contours for Blade 2 (volume fraction of 1.0 represents pure water and a volume fraction of 0.0 represents pure air).

Typical velocity vectors near the leading edge of a blade are shown in **Figure 6**. Most of the water layer adhering to the underside of the forming fabric is cleanly doctored by the blade. However, a fraction of the water is forced back between the fabrics, as indicated by the velocity vectors directed upwards. Some percentage of the underside water was forced back into the gap for both small and large nose radii.

Figure 7 shows the effect of nose radius on doctoring pressure distributions. For all cases, the peak doctoring pressure is about 50–60% of the stagnation pressure. For Blade 1, the doctoring pressure applies over a region about 1.5 mm upstream of the blade, which is about 2% of the distance over which the first pressure pulse applies upstream of the blade. As the nose radius increases, the doctoring pressure applies over a wider region upstream of the blade, and the location of the peak doctoring pressure ($x_{doc,max}$) shifts away from the leading edge of the blade. A larger nose radius also lets the fluid turn smoothly and reduces the peak negative pressure acting near the fabric–blade junction. For Blade 4, the doctoring pressure applies over a wider range than that of Blade 1. However, this range is still less than 3% of the range of the pressure pulse upstream of the blade. **Table IV** summarizes the effect of nose radius on doctoring pressure.

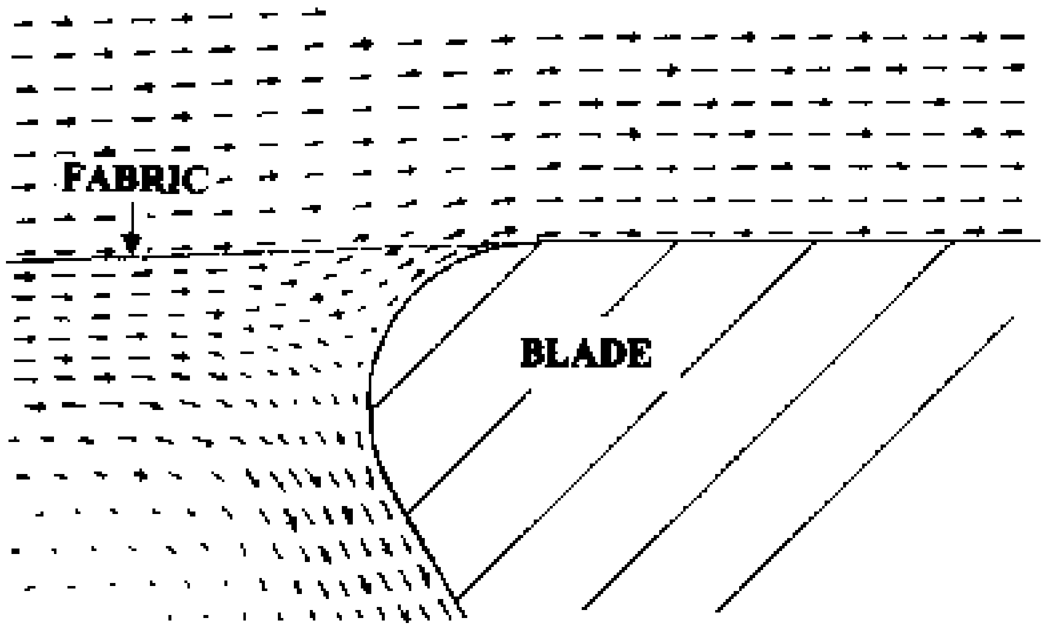

Figure 6. Velocity vectors near the blade tip for Blade 3. Some of the vectors are directed upwards, through the underside of the forming fabric (shown), which shows that a portion of the water adhering to the undersurface of the forming fabric is deflected back into the fabric.

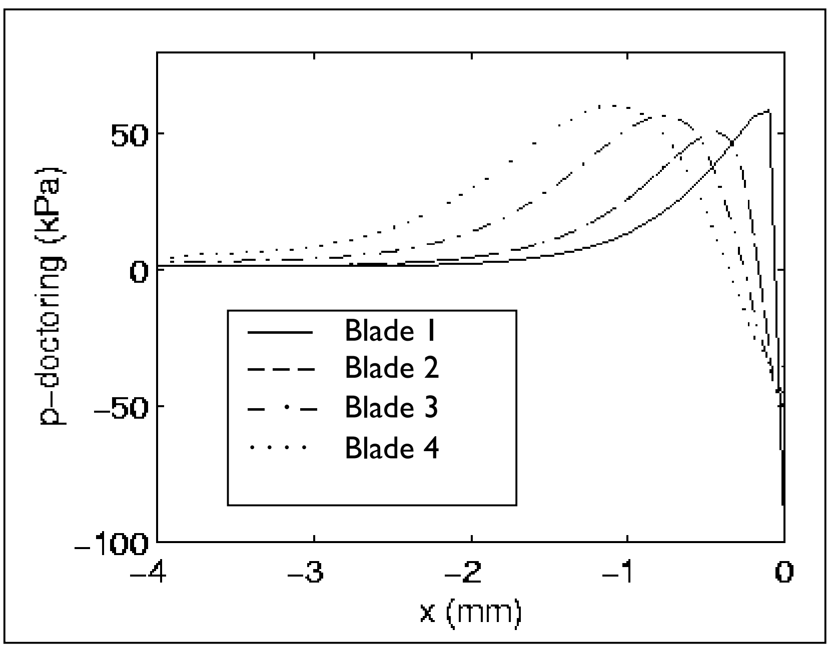

Figure 7. Effect of nose radius on doctoring pressure (x is the distance along the forming fabric, upstream of its contact point with the blade).

Blade No.	No. of cells	Peak doctoring pressure ($p_{doc,max}$), kPa	Location of peak doctoring pressure ($x_{doc,max}$), mm
1	7,600	60	–0.11
2	8,800	51	–0.43
3	9,970	57	–0.78
4	10,440	61	–1.12

Table IV. Summarized results of two-dimensional free-surface model.

2-D model of flow in the gap: Effect of doctoring on pressure pulses

Blade 1.

Figure 8 shows the pressure pulses in the gap at the bottom fabric p_b, in the middle p_m, and at the top fabric p_t. As expected, the effect of the doctoring pressure is important over a region a few millimeters upstream of the blade leading edge. As shown, the maximum pressure on the bottom fabric (8600 Pa) can exceed the pressure between the fabrics (in the middle, where the peak pressure is 6600 Pa) by as much as 30%. In addition, the pressure on the bottom fabric falls below atmospheric pressure (–3500 Pa for this case). This model also predicts a negative pressure on the bottom fabric just downstream of the trailing edge of the blade.

Blade 4.

Figure 9 shows pressure distributions in the gap for Blade 4, which has the largest radius of curvature at the blade leading edge. The maximum pressure at the bottom fabric can reach as high as 17,900 Pa, about 50% higher than the maximum pressure in the middle of the gap and more than double the peak pressure when doctoring does not occur. By subtracting the volume flow rate doctored down the blade surface from the volume flow rate on the undersurface of the forming fabric upstream of the blade, one can calculate the amount of water that is forced back into the fabric. For both Blades 1 and 4, about 10% of the water adhering to the underside of the fabric is forced back into the gap by the doctoring pressure.

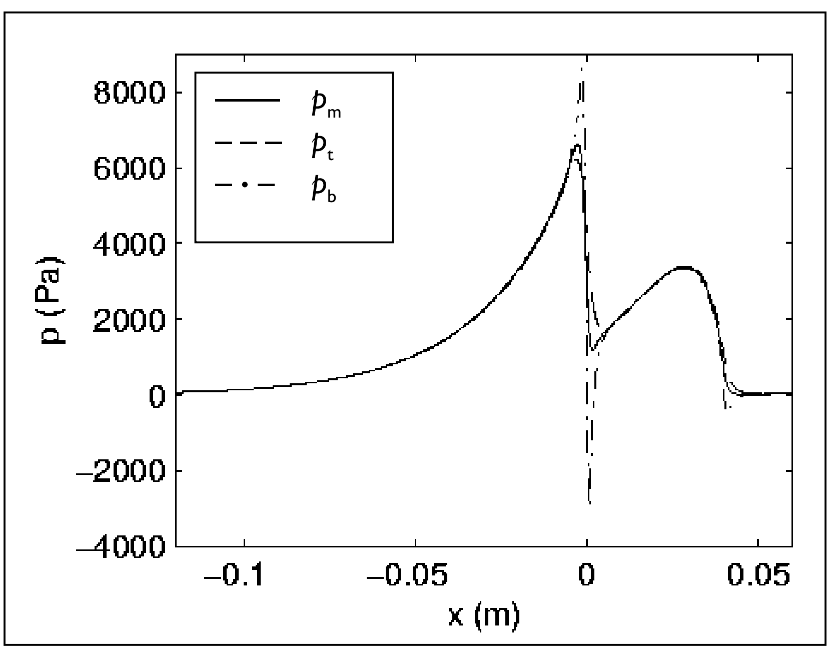

Figure 8. Pressure pulse in the gap for Blade 1.

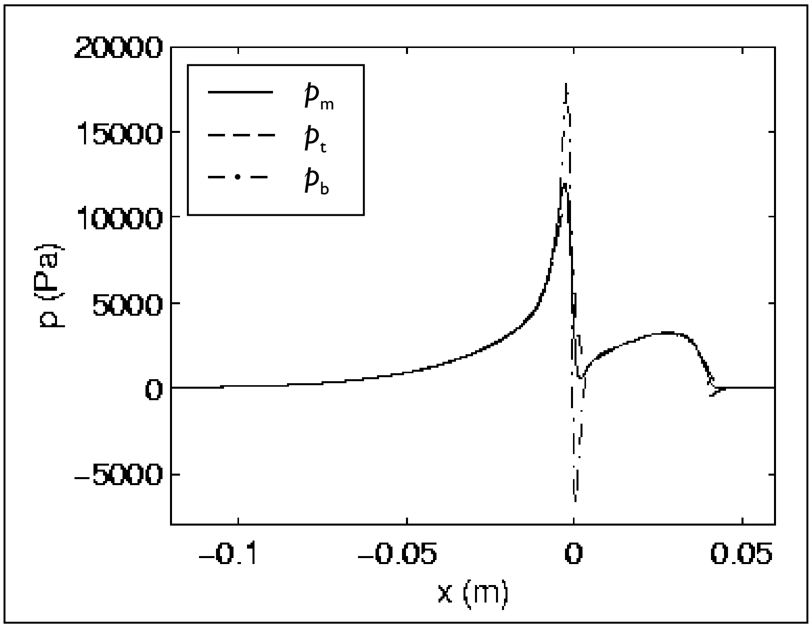

Figure 9. Pressure pulse in the gap for Blade 4.

A comparison between the pressure pulses in the middle of the gap, produced by different blades, is shown in **Figure 10**. As shown, the peak pressure in the gap increases with increasing nose radius. If the magnitude of the doctoring pressure were responsible for this increase in pressure pulse magnitude, then Blade 1 and Blade 4 should predict almost the same peak pressure (Blade 1 and Blade 4 produce doctoring pressures as high as 60 kPa, as seen in Table IV). As shown in Figure 7, with increasing nose radius, the location of maximum doctoring pressure shifts away from the leading edge of the blade and toward the location of the peak pressure pulse in the gap upstream of the blade. For example, for Blade 4, the location of the peak doctoring pressure (at –1.12 mm, as seen in Table IV) is the closest to the location of peak pressure pulse in the gap upstream of the blade (at –2.85 mm, as seen in **Table V**). Thus, this model predicts that the magnitude of the pressure pulse in the gap is affected more by the location of the peak doctoring pressure than by its magnitude.

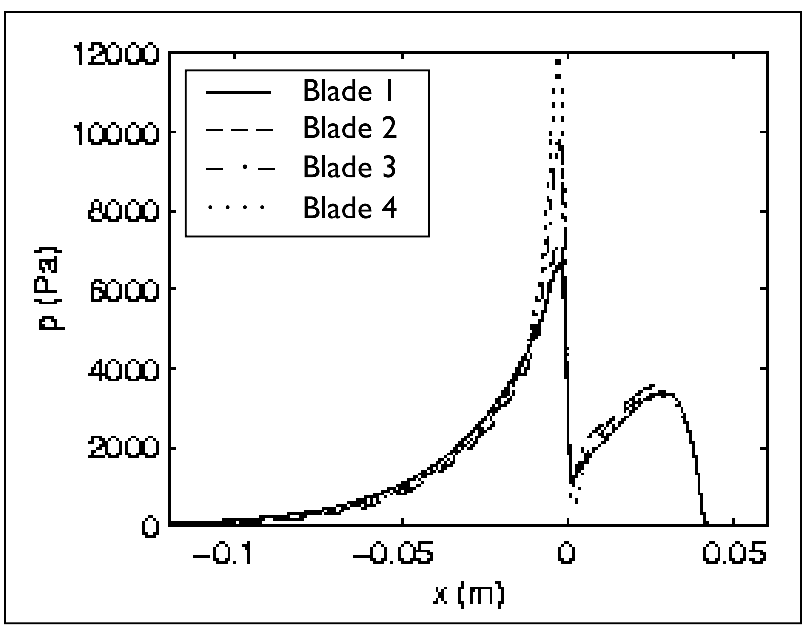

Figure 10. Pressure pulses in the middle of the gap.

Blade	No. of cells	$\int p_t\, dx$, Pa·m	Error, %	$p_{m,max}$, Pa	x_{max}, mm
1	109,200	287.2	2.9	6,640	–2.69
2	84,800	272.4	2.4	7,250	–2.74
3	84,800	298.4	6.7	9,770	–2.69
4	84,800	299.1	7.1	11,950	–2.85

Table V. Summarized results of the two-dimensional viscous model.

Figure 10 also shows that increasing the nose radius not only increases the peak pressure pulse right upstream of the leading edge of the blade, but it also decreases the pressure just downstream of the leading edge of the blade. It has been observed experimentally *(10)* that under some operating conditions, the water adhering to the top fabric is sucked back between the fabrics just downstream of the leading edge of the blade. This means that over this portion of the blade, the pressure of fluid at the top fabric drops below atmospheric pressure. The one-dimensional model of a single blade fails to predict any negative pressure over the blade. However, the two-dimensional free-surface model might predict negative pressures in the gap under some operating conditions. To investigate this possibility, some of the operating conditions given in Table I were modified, as seen in **Table VI**.

Tension on fabrics	5000 N/m
Velocity of fabric	14 m/s
Upstream wrap angle	1.2°
Downstream wrap angle	–0.2°
Blade width	50 mm

Table VI. Modified variables for simulation.

The pressure distributions at the top fabric obtained from different models are documented in **Figure 11**. As shown, the two-dimensional viscous model (without doctoring effect) predicts positive pressures all over the blade. However, if the doctoring effect is included, the two-dimensional model predicts the pressure at the top fabric is negative in a small region over the blade. Thus, water on the surface of the fabric would be sucked back through the top fabric. This phenomenon is believed to be likely to occur only when there is much more fabric wrap at the blade leading edge than at the blade trailing edge. This finding may explain an observation of Garner and Pye *(10)*, who found that, under some operating conditions, a small amount of water may be reabsorbed over the blade close to the leading edge.

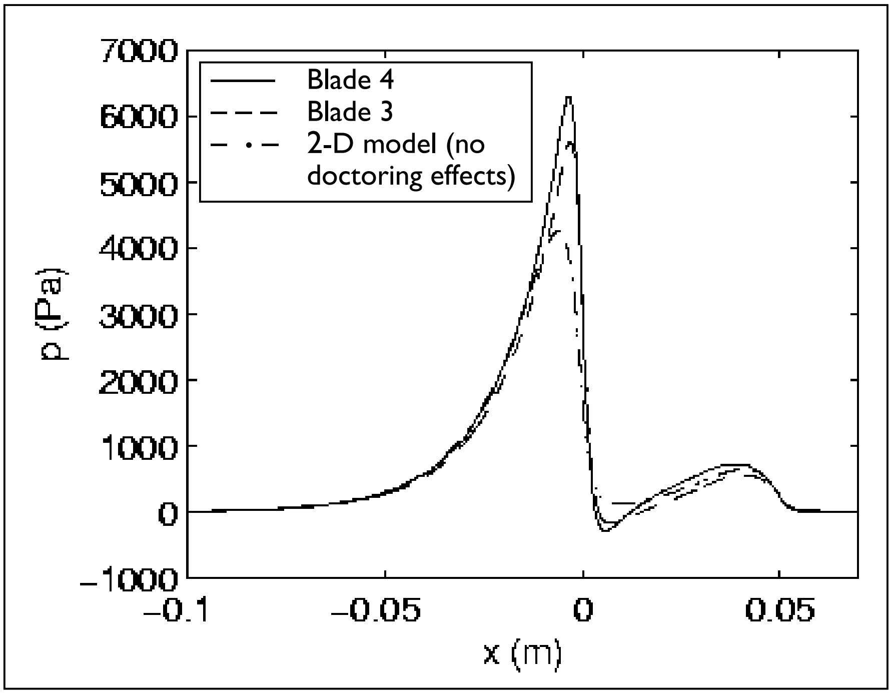

Figure 11. Pressure pulses at the top of the gap.

CONCLUSIONS

A numerical model of blade doctoring has been developed that combines a two-dimensional simulation of flow between the fabrics with a two-dimensional VOF (volume of fluid) model of the free surface impinging on the blade. The results show that the effect of the doctoring pressure is highly localized. The model predicts that, under typical operating conditions, the doctoring action causes the pressure in the water layer to reach its stagnation value some small distance down the blade front, away from the fabric–blade contact point. The amplitude of the doctoring pressure acting upon the lower fabric is less than the stagnation pressure, but it is high enough to cause a large pressure gradient within the gap just upstream of the blade.

The results further show that for commercial blade shapes, the nose radius has no significant effect on the maximum doctoring pressure. However, increasing the nose radius of curvature increases the distance over which the doctoring pressure applies, thereby significantly increasing the peak pressure pulse within the gap. The doctoring pressure forces a portion of the water, which was expelled from the gap upstream of the blade, back between the fabrics through the bottom fabric. Under some operating conditions, suction can be generated at the top fabric near where the fabrics wrap the leading edge of the blade. This suction can draw water between the fabrics that had previously been expelled through the top fabric.

Acknowledgement
The authors are grateful for the support they have received from AstenJohnson, Beloit, NSERC, and Paprican.

LITERATURE CITED

1. Zhao, R. H. and Kerekes, R. J., "Pressure distribution between forming fabrics in blade gap formers: Thin blade," *CPPA 80th Annnal Meeting Proceedings*, CPPA Technical Section, Montreal, 1994, pp. A32–38; *J. Pulp Paper Sci.* 21(3): 97(1995).
2. Green, S. I. and Kerekes, R. J., "Numerical analysis of pressure pulses induced by blades in gap formers," *TAPPI J.* 81(4): 180(1998).
3. Roshanzamir, A., Green, S. I., and Kerekes, R. J., "Two dimensional simulation of pressure pulses in blade gap formers," *J. Pulp Paper Sci.* 24(11): 364(1998).
4. Zahrai, S. and Bark, F. H., "An analysis of blade dewatering in a twin-wire paper machine," *J. Pulp Paper Sci.* 23(9): 452(1997).
5. Zahrai, S. and Bark, F. H., "On the fluid mechanics of twin wire blade forming in paper machines," *Nordic Pulp Paper Research J.* 10(4): 245(1995).
6. Green, S. I., "Modeling suction shoes in twin wire forming: Theory," *TAPPI J.* 82(9): 136(1999).
7. Norman, B., "Principles of twin-wire forming," *Svensk Papperstid.* 82(11): 330(1979).
8. Fluent User's Manual, "*VOF Free Surface Model*," Vol. 2, Chap. 10, Creare.x, Hanover, NH, 1996.
9. Appel, D. W. and Yu, Y. S., "Free-streamline analyses of flow from nozzles, flow through side inlets, and flow past corners," Report No. 17, University of Kansas, Lawrence, 1963, pp. 19–23.
10. Garner, R. G. and Pye, I. T., "High-speed forming," Paprican internal report, PAPRICAN, Pointe Claire, PQ, 1985, pp. 86–89.

Received: November 9, 2000
Revised: February 16, 2001
Accepted: February 21, 2001

This paper was accepted for abstracting and publication in the July 2001 issue of *TAPPI JOURNAL.*

TAPPI Website: www.tappi.org